

Zittlau, 1983; Becker, Cohen-Addad, Delley, Hirshfeld & Lehmann, 1986). The deformation density along the S(2)—S(3) bond is peculiar and quite similar to the S—S—S region in thiathiophthene (Wang, Chen & Wu, 1988). This may be rationalized by recent MO calculations (Kunze & Hall, 1986, 1987) which showed that a valence-electron-rich atom like O, S or F tends to have little density accumulation in the bonding region, if the spherical atomic model density is subtracted.

The authors would like to thank Mr Karl H. Claus of the Max-Planck-Institute für Kohlenforschung for his help on low-temperature data collection. Thanks are due to the National Science Council for the support of this work.

References

BECKER, P., COHEN-ADDAD, C., DELLEY, B., HIRSHFELD, F. L. & LEHMANN, M. S. (1986). *Applied Quantum Chemistry*, edited by V. H. SMITH JR, H. F. SCHAEFER III & K. MOROKUMA, pp. 361–373. Dordrecht: D. Reidel.

BREITENSTEIN, M., DANNOHL, H., MEYER, H., SCHWEIG, A., SEEGER, R., SEEGER, U. & ZITTLAU, W. (1983). *Int. Rev. Phys. Chem.* **3**, 335–391.
 BUSING, W. R. & LEVY, H. A. (1964). *Acta Cryst.* **17**, 142–146.
 COHEN-ADDAD, C., LEHMANN, M. & BECKER, P. (1984). *J. Chem. Soc. Perkin Trans. 2*, pp. 191–196.
 CUMMINGS, A. D. & SIMMONS, H. E. (1928). *Ind. Eng. Chem.* **20**, 1173–1176.
 DUNITZ, J. D. & SEILER, P. (1983). *J. Am. Chem. Soc.* **105**, 7056–7058.
 KARLE, I. L., ESTLIN, J. A. & BRITTS, K. (1967). *Acta Cryst.* **22**, 273–280.
 KUNZE, K. L. & HALL, M. B. (1986). *J. Am. Chem. Soc.* **108**, 5122–5127.
 KUNZE, K. L. & HALL, M. B. (1987). *J. Am. Chem. Soc.* **109**, 7617–7623.
 WANG, Y., BLESSING, R. H., ROSS, F. & COPPENS, P. (1976). *Acta Cryst.* **B32**, 572–578.
 WANG, Y., CHEN, M. J. & WU, C. H. (1988). *Acta Cryst.* **B44**, 179–182.
 WANG, Y., GUO, L. W., LIN, H. C., KAO, C. T., TSAI, C. J. & BATS, J. W. (1988). *Inorg. Chem.* **27**, 520–524.
 WANG, Y., LIAO, J. H. & UENG, C. H. (1986). *Acta Cryst.* **C42**, 1420–1423.
 WANG, Y., TSAI, C. J., LIU, W. L. & CALVERT, L. D. (1985). *Acta Cryst.* **B41**, 131–135.

Acta Cryst. (1989). **B45**, 69–77

Crystallochromy as a Solid-State Effect: Correlation of Molecular Conformation, Crystal Packing and Colour in Perylene-3,4,9,10-bis(dicarboximide) Pigments

BY GERHARD KLEBE, FRITZ GRASER, ERICH HÄDICKE AND JÜRGEN BERNDT

Hauptlaboratorium, Farbenlaboratorium and Ammoniaklaboratorium of BASF Aktiengesellschaft, D-6700 Ludwigshafen, Federal Republic of Germany

(Received 27 January 1988; accepted 22 August 1988)

Dedicated to Professor Dr Helmut Dörfel on the occasion of his 60th birthday

Abstract

The crystal structure determination of four pigments is described and their structures compared with those of 14 related perylenes. Crystal data: *N,N'*-bis(4-hydroxybutyl)perylene-3,4,9,10-bis(dicarboximide), $C_{32}H_{26}N_2O_6$, $P\bar{1}$, $a = 4.705$ (1), $b = 15.002$ (4), $c = 18.591$ (4) Å, $\alpha = 109.72$ (2), $\beta = 95.74$ (2), $\gamma = 92.82$ (2)°, $Z = 2$, $D_x = 1.450$ g cm⁻³, $R(F) = 0.078$ for 2578 reflections; *N,N'*-bis(6-hydroxyhexyl)perylene-3,4,9,10-bis(dicarboximide), $C_{36}H_{34}N_2O_6$, $P\bar{1}$, $a = 4.739$ (3), $b = 17.412$ (14), $c = 18.991$ (11) Å, $\alpha = 65.24$ (5), $\beta = 88.42$ (5), $\gamma = 85.82$ (7)°, $Z = 2$, $D_x = 1.382$ g cm⁻³, $R(F) = 0.107$ for 1588 reflections; *N,N'*-bis(4-ethoxyphenyl)perylene-3,4,9,10-bis(dicarboximide), $C_{40}H_{26}N_2O_6$, $P\bar{1}$, $a = 4.934$ (1), $b = 15.915$ (4), $c = 18.849$ (9) Å, $\alpha = 100.17$ (3), $\beta = 95.89$ (3), $\gamma = 93.50$ (2)°, $Z = 2$, $D_x = 1.450$ g cm⁻³,

$R(F) = 0.070$ for 2268 reflections; *N,N'*-bis(4-phenylazophenyl)perylene-3,4,9,10-bis(dicarboximide), $C_{48}H_{26}N_6O_4$, $P\bar{1}$, $a = 5.291$ (1), $b = 11.865$ (2), $c = 13.972$ (2) Å, $\alpha = 102.35$ (1), $\beta = 97.32$ (1), $\gamma = 92.71$ (1)°, $Z = 1$, $D_x = 1.471$ g cm⁻³, $R(F) = 0.046$ for 1716 reflections. Differently substituted perylene-3,4,9,10-bis(dicarboximide) pigments show closely related absorption spectra in a molecular dispersion such as in polystyrene. In the crystalline state the absorption maxima of the same series of compounds spread over a range of more than 170 nm. This crystallochromic solid-state effect is due to different packings of the individual dye molecules in the crystal, in which the molecules are arranged in stacks. All molecules possess a flat perylene tetracarboxylic diimide moiety with bent side-chain substituents. The steric requirement, the crystal conformation and the mutual interlocking of these substituents is classified

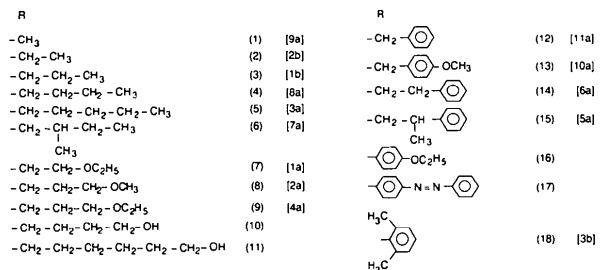
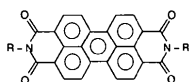
0108-7681/89/010069-09\$03.00

© 1989 International Union of Crystallography

and related to crystal packing. An empirical correlation between crystal-packing parameters and absorption properties is found. Reliable prediction of crystal packing and thus pigment colour from the topology and structure of an isolated dye molecule could not be achieved.

Introduction

The colouring of organic dyes is mainly determined by the electronic properties of the individual molecules which compose the dyestuff. However, in the solid state the absorption characteristics of the isolated molecular chromophore could be dramatically influenced and modified by the electronic interactions of the close-packed molecules. This effect of solid-state 'crystallochromy' is clearly indicated and well established for a series of substituted perylene-3,4:9,10-bis-(dicarboximide) pigments (1)–(18) (Graser & Hädicke, 1980, 1984; Hädicke & Graser, 1986*a,b*).



The numbering scheme in square brackets refers to the numbering in the previous papers: [1a to 11a] Hädicke & Graser (1986*a*), [1b to 3b] Hädicke & Graser (1986*b*).

In a molecular dispersion of these pigments, *e.g.* in polystyrene, where any short-range interactions of two perylene chromophores might be excluded, all investigated compounds show rather closely related absorption spectra composed of three major absorptions at approximately 530, 490 and 460 nm. In the crystalline phase the absorption maxima of the same series of compounds spread over a range of more than 170 nm. Furthermore the overall shape of the absorption bands is appreciably different.

This crystallochromic solid-state effect is related to differences in the packing of the individual dye molecules in the different pigments. In order to correlate the crystallographic packing parameters with the colour of the particular pigment, we embarked on a systematic study of the crystal structures of differently substituted perylenes. Up to now, 24 different packing patterns have been detected in the solid state. All the investigated compounds, (1)–(18), have a planar perylenetetra-

Table 1. *Crystal data and experimental details for (10), (11), (16) and (17)*

Formula	(10)		(11)		(16)		(17)	
	C ₁₃ H ₂₈ N ₂ O ₆		C ₁₆ H ₁₄ N ₂ O ₆		C ₄₀ H ₂₈ N ₂ O ₆		C ₄₈ H ₂₈ N ₂ O ₄	
Solvent for crystallization	Nitrobenzene		Nitrobenzene		Nitrobenzene		Nitrobenzene	
Elementary analysis (%)	Calc.	Obs.	Calc.	Obs.	Calc.	Obs.	Calc.	Obs.
C	71.9	72.2	73.2	72.8	76.2	75.3	76.8	75.9
H	4.9	4.9	5.8	5.9	4.1	4.3	3.5	3.7
N	5.2	5.3	4.7	4.7	4.4	4.4	11.2	11.1
O	18.0	17.9	16.3	16.9	15.2	15.6	8.5	9.2
<i>a</i> (Å)	4.705 (1)		4.739 (3)		4.934 (1)		5.291 (1)	
<i>b</i> (Å)	15.002 (4)		17.412 (14)		15.915 (4)		11.865 (2)	
<i>c</i> (Å)	18.591 (4)		18.991 (11)		18.849 (9)		13.972 (2)	
α (°)	109.72 (2)		65.24 (5)		100.17 (3)		102.35 (1)	
β (°)	95.74 (2)		88.42 (5)		95.89 (3)		97.32 (1)	
γ (°)	92.82 (2)		85.82 (7)		93.50 (2)		92.71 (1)	
Absorption coefficient (cm ⁻¹)	7.84		7.25		7.58		7.35	
Density (g cm ⁻³)	1.450		1.382		1.450		1.471	
Z	2		2		2		1	
<i>V</i> (Å ³)	1224.3		1419.2		1444.4		847.3	

carboxylic diimide moiety in common. At the two N atoms they bear differently bent side chains which can be grouped into linear and branched alkyl [(1)–(6)], alkyl ether [(7)–(9)] and alkyl alcohol [(10), (11)] groups, alkyl aromatics bound through an aliphatic C atom to the perylene system [(12)–(15)] and aromatic groups directly connected to the chromophore [(16)–(18)]. The mutual arrangement of the neighbouring molecules (mainly in stacks) in the crystal is determined by these substituents. As a consequence, the geometrical overlap of the perylene systems of neighbouring molecules varies within the series and the intermolecular interactions between the vicinal chromophores which affect the colour of the pigment are modified.

In the present contribution the crystal structures of four perylenes, (10), (11), (16), (17), are discussed and compared. The solid-state colour of all 18 pigments is correlated with the geometrical packing parameters by means of an empirically derived equation. An attempt is made to predict crystal packing from the molecular conformation of the individual molecules.

Experimental

The spectroscopic measurements, sample preparation and crystal growth of (10) and (11) were performed as described by Graser & Hädicke (1980). Crystals of (16) and (17) were obtained from solution at approximately 463 K within a small temperature gradient over several days. The λ_{max} values were derived from the spectroscopic data as depicted earlier (Graser & Hädicke, 1984). The solvent used for crystallization, the elementary analyses and further physical properties are given in Table 1. To exclude any differences in solid-state modifications between the single crystals (structure determination) and the powder samples (spectroscopy, crystal growth) Debye–Scherrer diagrams were recorded.

Nicolet P2, diffractometer with monochromated Cu K α radiation, crystal sizes: (10) 0.45 \times 0.20 \times 0.13 mm, (11) 0.45 \times 0.05 \times 0.01 mm, (16) 0.54 \times 0.09 \times 0.07 mm, (17) 0.48 \times 0.12 \times 0.06 mm. The lattice parameters (Table 1) were refined from the angular settings of 25 strong reflections up to $2\theta = 35^\circ$. In all four cases a triclinic unit cell was found and intensity statistics (Wilson, 1949) indicated the centrosymmetric space group $P\bar{1}$. Data were collected at room temperature up to $2\theta = 115^\circ$ in $\theta/2\theta$ scan mode (scan width 1.10–1.75 $^\circ$), resulting in (10) 3126, (11) 3568, (16) 3711 and (17) 2143 reflections. Range of hkl in all cases $h \pm k \pm l$. A standard reflection was recorded every 100 min, no significant fluctuations, no correction for absorption, correction for Lorentz and polarization effects. After background correction according to an algorithm of Lehmann & Larsen (1974) (see also Blessing, Coppens & Becker, 1974) by the program LAUSANNE (Schwarzenbach, 1977) and averaging over symmetry equivalent reflections, sets of (10) 3102, (11) 3568, (16) 3711 and (17) 2143 unique reflections were used for structure determination of which (10) 542, (11) 1980, (16) 1443 and (17) 427 reflections were flagged as unobserved [criterion $4\sigma(F)$; in (10) $2\sigma(F)$].

All structures were solved by direct methods using the SHELXTL package (Sheldrick, 1978) on a Data General Eclipse S/200. In (17) the asymmetric unit is half a molecule, and the complete moiety is generated by inversion at the centroid of the central benzene ring. In (10), (11) and (16) two independent halves are present in the asymmetric unit and possess slightly different conformations. As in (17) they are completed by inversion symmetry. Structure refinement was performed with a least-squares block-cascade algorithm (Sheldrick, 1978). H-atom positions were found by difference Fourier synthesis. They were included in the structure model in idealized geometry and constrained to give C–H 0.96 Å, H–C–H 109.5 $^\circ$, rigid CH₃ groups, riding CH₂ and CH groups with equal C–C–H angles. Anisotropic temperature factors were applied for C, N and O atoms; the H atoms were treated with isotropic thermal parameters. In all cases the function minimized was $\sum w(|F_o - F_c|^2)$ where the weights w are calculated based on counting statistics with a term g included for random errors: $w = [\sigma^2(F) + gF^2]^{-1}$, with g for (10) 0.0035, (11) 0.0017, (16) 0.0022 and (17) 0.0011.

Convergence was achieved and a weighting scheme was applied to obtain a flat variance in terms of $\sin\theta/\lambda$ and the magnitude of F_o . Scattering factors were taken from *International Tables for X-ray Crystallography* (1974). (10) $R(F) = 0.078$, $wR(F) = 0.086$ for 2578 reflections, (11) $R(F) = 0.107$, $wR(F) = 0.106$ for 1588 reflections, (16) $R(F) = 0.070$, $wR(F) = 0.076$ for 2268 reflections and (17) $R(F) = 0.046$, $wR(F) = 0.054$ for 1716 reflections. Δ/σ_{\max} for (10) 0.06, (11) 0.08, (16)

Table 2. Atomic coordinates ($\times 10^4$) and equivalent isotropic temperature factors ($\text{\AA}^2 \times 10^3$) of (10)

	x	y	z	U_{eq}
C(1)	6579 (8)	9705 (3)	5576 (2)	40 (1)
C(2)	6761 (8)	9232 (2)	4777 (2)	41 (1)
C(3)	5209 (8)	9507 (3)	4194 (2)	43 (1)
C(4)	5441 (9)	9001 (3)	3428 (2)	52 (2)
C(5)	7173 (9)	8256 (3)	3221 (2)	53 (2)
C(6)	8692 (8)	7981 (3)	3766 (2)	43 (1)
C(7)	8518 (8)	8462 (2)	4552 (2)	41 (1)
C(8)	10061 (8)	8184 (3)	5117 (2)	47 (2)
C(9)	9814 (9)	8643 (3)	5880 (2)	55 (2)
C(10)	8119 (9)	9397 (3)	6107 (2)	52 (2)
C(11)	11896 (9)	7387 (3)	4891 (2)	51 (2)
C(12)	10466 (9)	7170 (3)	3532 (2)	50 (2)
N(1)	11977 (7)	6928 (2)	4108 (2)	46 (1)
O(1)	13267 (7)	7120 (2)	5358 (2)	72 (1)
O(2)	10585 (7)	6714 (2)	2857 (2)	67 (1)
C(13)	13719 (9)	6109 (3)	3881 (3)	55 (2)
C(14)	12013 (9)	5171 (3)	3778 (3)	58 (2)
C(15)	13765 (10)	4332 (3)	3538 (3)	61 (2)
C(16)	12059 (11)	3409 (3)	3432 (3)	74 (2)
O(3)	13611 (10)	2601 (3)	3156 (2)	100 (2)
C(21)	1826 (8)	5319 (2)	729 (2)	38 (1)
C(22)	2048 (7)	4405 (2)	168 (2)	36 (1)
C(23)	268 (8)	4072 (2)	551 (2)	38 (1)
C(24)	622 (8)	3171 (3)	-1070 (2)	43 (2)
C(25)	2621 (8)	2607 (3)	898 (2)	45 (2)
C(26)	4352 (8)	2911 (2)	-208 (2)	42 (1)
C(27)	4080 (8)	3812 (2)	341 (2)	39 (1)
C(28)	5840 (8)	4134 (2)	1052 (2)	40 (1)
C(29)	5614 (8)	5012 (3)	1579 (2)	46 (2)
C(30)	3631 (8)	5601 (3)	1417 (2)	44 (1)
C(31)	7971 (9)	3524 (3)	1232 (2)	48 (2)
C(32)	6459 (9)	2292 (3)	-30 (2)	46 (2)
N(21)	8114 (7)	2632 (2)	678 (2)	46 (1)
O(21)	9537 (7)	3778 (2)	1838 (2)	64 (1)
O(22)	6707 (6)	1500 (2)	-484 (2)	58 (1)
C(33)	10135 (8)	2003 (3)	876 (3)	51 (2)
C(34)	8744 (9)	1366 (3)	1243 (2)	52 (2)
C(35)	10834 (9)	732 (3)	1452 (3)	55 (2)
C(36)	9456 (9)	42 (3)	1763 (3)	57 (2)
O(23)	11387 (7)	565 (2)	1955 (2)	66 (1)

0.11 and (17) 0.06; max. heights in final difference Fourier synthesis (10) 0.33, (11) 0.46, (16) 0.24, and (17) 0.18 e Å⁻³.

Discussion of the crystal structures

Final atomic positions and U_{eq} 's for the non-H atoms are given in Tables 2–5 using the labelling scheme indicated in Figs. 1–4.* In (10), (11) and (16) two independent halves of the molecules, located on an inversion centre, form the asymmetric unit. They give rise to two different stacking patterns in the crystal. A slight deviation in conformation between the two independent halves arises from differences in the torsion angles of the substituents. In (10) and (11) the (CH₂)_nOH ($n = 4, 6$) group possesses an all-*trans* conformation. The packing in the unit cell (Figs. 5–7) for (10) and (11) is related. The mutual orientation of

* Lists of structure factors, anisotropic thermal parameters, H-atom parameters, and bond distances and angles of the four compounds have been deposited with the British Library Document Supply Centre as Supplementary Publication No. SUP 51267 (71 pp.). Copies may be obtained through The Executive Secretary, International Union of Crystallography, 5 Abbey Square, Chester CH1 2HU, England.

Table 3. Atomic coordinates ($\times 10^4$) and equivalent isotropic temperature factors ($\text{\AA}^2 \times 10^3$) of (11)

$U_{eq} = \frac{1}{3}$ (trace of the orthogonalized U_{ij} tensor).

	x	y	z	U_{eq}
C(1)	1523 (20)	107 (6)	601 (6)	39 (5)
C(2)	1843 (22)	655 (6)	-183 (7)	41 (5)
C(3)	406 (21)	587 (6)	-805 (6)	32 (5)
C(4)	832 (22)	1147 (7)	-1570 (6)	44 (6)
C(5)	2626 (23)	1804 (7)	-1741 (6)	48 (6)
C(6)	4042 (22)	1897 (7)	-1155 (7)	43 (6)
C(7)	3727 (22)	1330 (7)	-375 (7)	47 (6)
C(8)	5103 (19)	1444 (6)	206 (6)	33 (5)
C(9)	4721 (21)	904 (6)	964 (6)	40 (5)
C(10)	2892 (21)	254 (6)	1167 (6)	46 (5)
C(11)	7072 (21)	2139 (6)	-3 (7)	46 (6)
C(12)	5986 (21)	2609 (6)	-1385 (6)	45 (6)
N(1)	7289 (17)	2686 (5)	-782 (6)	44 (5)
O(1)	8376 (15)	2235 (5)	505 (5)	61 (4)
O(2)	6210 (16)	3121 (5)	-2037 (4)	62 (4)
C(13)	9088 (24)	3413 (6)	-969 (7)	56 (6)
C(14)	7388 (24)	4155 (6)	-954 (7)	51 (6)
C(15)	9097 (24)	4925 (6)	-1125 (6)	52 (6)
C(16)	7370 (23)	5702 (7)	-1208 (7)	60 (7)
C(17)	8998 (25)	6497 (6)	-1441 (7)	67 (7)
C(18)	7253 (27)	7278 (7)	-1624 (8)	79 (7)
O(3)	8761 (20)	8031 (5)	-1862 (4)	73 (4)
C(21)	8597 (20)	-666 (6)	5597 (6)	38 (5)
C(22)	8163 (21)	-500 (6)	4821 (6)	38 (4)
C(23)	9470 (21)	173 (6)	4189 (6)	40 (5)
C(24)	8999 (21)	294 (7)	3429 (6)	43 (6)
C(25)	7169 (23)	-189 (7)	3261 (7)	51 (6)
C(26)	5882 (22)	-832 (7)	3863 (8)	49 (7)
C(27)	6276 (21)	-1003 (7)	4635 (8)	45 (7)
C(28)	4893 (21)	-1650 (6)	5255 (7)	37 (6)
C(29)	5401 (23)	-1799 (7)	5992 (7)	49 (6)
C(30)	7240 (23)	-1327 (7)	6177 (6)	48 (6)
C(31)	2860 (22)	-2133 (7)	5038 (6)	52 (6)
C(32)	3926 (20)	-1348 (6)	3632 (5)	28 (4)
N(21)	2574 (16)	-1973 (5)	4270 (5)	45 (5)
O(21)	1721 (16)	-2722 (5)	5539 (4)	66 (4)
O(22)	3579 (16)	-1245 (5)	2974 (4)	61 (4)
C(33)	870 (23)	-2534 (6)	4072 (7)	51 (5)
C(34)	2548 (22)	-3304 (6)	4075 (7)	53 (6)
C(35)	819 (24)	-3882 (7)	3872 (7)	59 (7)
C(36)	2592 (25)	-4619 (7)	3819 (7)	65 (7)
C(37)	965 (27)	-5148 (7)	3508 (8)	76 (8)
C(38)	2770 (30)	-5789 (8)	3397 (10)	109 (11)
O(23)	1222 (28)	-6276 (7)	3123 (6)	122 (7)

Table 4. Atomic coordinates ($\times 10^4$) and equivalent isotropic temperature factors ($\text{\AA}^2 \times 10^3$) of (16)

$U_{eq} = \frac{1}{3}$ (trace of the orthogonalized U_{ij} tensor).

	x	y	z	U_{eq}
C(1)	3066 (4)	4338 (2)	10342 (2)	34 (1)
C(2)	4265 (4)	3818 (2)	9521 (2)	33 (1)
C(3)	6184 (4)	4449 (2)	9155 (2)	35 (1)
C(4)	7231 (5)	3893 (2)	8345 (2)	42 (1)
C(5)	6567 (5)	2733 (2)	7893 (2)	43 (1)
C(6)	4768 (4)	2101 (2)	8241 (2)	36 (1)
C(7)	3576 (4)	2639 (2)	9048 (2)	34 (1)
C(8)	1658 (4)	2008 (2)	9380 (2)	36 (1)
C(9)	510 (5)	2530 (2)	10167 (2)	42 (1)
C(10)	1203 (5)	3682 (2)	10643 (2)	41 (1)
C(11)	879 (5)	794 (2)	8877 (2)	40 (1)
C(12)	4171 (4)	869 (2)	7771 (2)	38 (1)
N(1)	2367 (4)	266 (1)	8170 (1)	39 (1)
O(1)	-934 (4)	248 (1)	9064 (1)	51 (1)
O(2)	5158 (3)	373 (1)	7076 (1)	49 (1)
C(13)	1952 (5)	-975 (2)	7785 (2)	40 (1)
C(14)	3798 (5)	-1663 (2)	8071 (2)	45 (1)
C(15)	3417 (5)	-2849 (2)	7717 (2)	46 (1)
C(16)	1224 (5)	-3330 (2)	7089 (2)	39 (1)
C(17)	-619 (5)	-2624 (2)	6812 (2)	47 (1)
C(18)	-241 (5)	-1447 (2)	7161 (2)	47 (1)
N(2)	1022 (4)	-4567 (2)	6780 (2)	46 (1)
N(3)	-859 (4)	-4974 (2)	6147 (2)	45 (1)
C(19)	-1048 (5)	-6211 (2)	5847 (2)	41 (1)
C(20)	805 (5)	-6908 (2)	6136 (2)	48 (1)
C(21)	392 (5)	-8096 (2)	5812 (2)	53 (1)
C(22)	-1826 (6)	-8584 (2)	5207 (2)	55 (1)
C(23)	-3636 (5)	-7892 (2)	4918 (2)	57 (1)
C(24)	-3259 (5)	-6706 (2)	5232 (2)	52 (1)

Table 5. Atomic coordinates ($\times 10^4$) and equivalent isotropic temperature factors ($\text{\AA}^2 \times 10^3$) of (17)

$U_{eq} = \frac{1}{3}$ (trace of the orthogonalized U_{ij} tensor).

	x	y	z	U_{eq}
C(1)	6798 (9)	4314 (3)	-101 (2)	42 (2)
C(2)	4971 (8)	4454 (3)	-693 (2)	39 (2)
C(3)	3189 (9)	5134 (3)	-607 (2)	44 (2)
C(4)	1529 (10)	5253 (3)	-1213 (2)	52 (2)
C(5)	1424 (10)	4714 (3)	-1882 (2)	51 (2)
C(6)	3071 (9)	4046 (3)	-1968 (2)	45 (2)
C(7)	4871 (8)	3917 (3)	-1377 (2)	40 (2)
C(8)	6637 (9)	3238 (3)	-1474 (2)	43 (2)
C(9)	8406 (10)	3124 (3)	-898 (2)	51 (2)
C(10)	8513 (9)	3652 (3)	-220 (2)	49 (2)
C(11)	6530 (10)	2659 (3)	-2182 (3)	52 (2)
C(12)	2941 (9)	3474 (3)	-2673 (2)	48 (2)
N(1)	4667 (7)	2810 (2)	-2743 (2)	50 (1)
O(1)	8011 (8)	2073 (2)	-2282 (2)	71 (2)
O(2)	1327 (6)	3562 (2)	-3190 (2)	57 (1)
C(13)	4372 (9)	2228 (3)	-3435 (2)	45 (2)
C(14)	2286 (10)	1587 (3)	-3602 (2)	51 (2)
C(15)	1905 (10)	1070 (3)	4267 (2)	48 (2)
C(16)	3613 (10)	1193 (3)	-4794 (2)	48 (2)
C(17)	5754 (10)	1806 (3)	-4619 (2)	49 (2)
C(18)	6141 (10)	2328 (3)	-3943 (2)	49 (2)
O(3)	2945 (7)	672 (2)	-5453 (2)	59 (1)
C(19)	4557 (11)	784 (3)	-6028 (2)	60 (2)
C(20)	3208 (13)	221 (4)	-6709 (3)	85 (3)
C(21)	-822 (10)	5857 (3)	-4824 (2)	49 (2)
C(22)	1323 (9)	5581 (3)	-4371 (2)	46 (2)
C(23)	2197 (9)	4745 (3)	-4546 (2)	48 (2)
C(24)	4428 (10)	4520 (3)	-4119 (2)	53 (2)
C(25)	5630 (11)	5088 (3)	-3499 (3)	59 (2)
C(26)	4714 (10)	5887 (3)	-3304 (2)	53 (2)
C(27)	2584 (9)	6144 (3)	-3748 (2)	48 (2)
C(28)	1743 (10)	6980 (3)	-3575 (2)	54 (2)
C(29)	-241 (10)	7257 (3)	-4029 (3)	63 (2)
C(30)	-1473 (11)	6704 (3)	-4646 (3)	60 (2)
C(31)	2863 (11)	7559 (4)	-2898 (3)	57 (2)
C(32)	5912 (11)	6443 (3)	-2623 (3)	62 (2)
N(21)	4839 (9)	7239 (3)	-2440 (2)	61 (2)
O(21)	2198 (8)	8282 (2)	-2724 (2)	73 (2)
O(22)	7752 (8)	6241 (2)	-2224 (2)	90 (2)
C(33)	5606 (11)	7721 (3)	-1712 (2)	59 (2)
C(34)	4228 (17)	7547 (4)	-1169 (3)	117 (3)
C(35)	4902 (16)	7999 (4)	-462 (3)	124 (4)
C(36)	6924 (11)	8615 (4)	-310 (3)	73 (2)
C(37)	8224 (14)	8836 (4)	-865 (3)	103 (3)
C(38)	7568 (13)	8386 (4)	-1566 (3)	92 (3)
O(23)	7714 (8)	9090 (3)	362 (2)	95 (2)
C(39)	6249 (15)	8954 (4)	944 (3)	98 (3)
C(40)	7530 (16)	9489 (4)	1627 (3)	113 (3)

the two symmetry-independent stacks in the crystal is not parallel, best planes through the atoms of the perylene moieties within the stacks are inclined at 26° in (10) (Fig. 7) and only at $6\text{--}7^\circ$ in (11). In the *bc* projection plane the angle between the longitudinal axis through molecules belonging to differently oriented stacks is similar in (10) and (11) (see Figs. 5, 6). In the first of the two crystal conformers of (16), a best plane through the atoms of the phenyl ring is twisted by $81\text{--}7^\circ$ out of a plane through the perylene system: in the second by $84\text{--}4^\circ$. Whereas in the first the bisecting vector through the phenyl ring deviates only $6\text{--}1^\circ$ from a corresponding vector through the perylene portion, this inclination is more than twice as large in the latter ($13\text{--}3^\circ$). In both examples the ethoxy group is nearly coplanar with the phenyl ring ($\tau = 7\text{--}2, 9\text{--}4^\circ$). In the *bc* projection plane the two independent stacks are oriented nearly parallel (Fig. 8). Best planes through the atoms of the perylene moieties are inclined at $21\text{--}3^\circ$ to each other. In (17) the asymmetric unit consists of half

a molecule, the complete framework being generated by inversion symmetry. The azobenzene moiety is nearly planar (interplanar angle 1.9°), but twisted by 75.9° out of a plane through the perylene system. A slight inclination of the substituent relative to the perylene moiety is indicated by an angle of 9.3° between the bisecting vector through the perylene and azobenzene parts of the molecule. The orientation of the stacks in the crystal is shown in Fig. 9.

The intermolecular distances within each stack are discussed in the following section. The bond distances and angles in the molecules are in the range normally observed for organic compounds.

Correlation of crystal packing with pigment colour and molecular conformation

The colour of a pigment is not only determined by the electronic properties of the individual molecular chromophores but is also influenced by the electronic interactions with the vicinal molecules in the crystal. In molecules (1)–(18) 24 distinct packing patterns are

observed, where the central perylene moiety is embedded in different environments (Fig. 10). In all cases the molecules arrange in stacks showing a parallel orientation of the flat perylene moiety. Graphite serves as a reference compound with a stacked arrangement of fused aromatic rings. Infinite planes of six-membered rings stack with an interlayer distance of 3.35 \AA . A relative 'longitudinal' shift of 1.14 \AA between two vicinal layers is observed; perpendicular, no 'transverse' shift is found. Thus, a C atom of an upper layer is located on the centre of a ring in the lower layer. With the exception of (18), the stacking distance (Fig. 10) between neighbouring perylene moieties is $3.34\text{--}3.55 \text{ \AA}$, rather close to that in graphite.

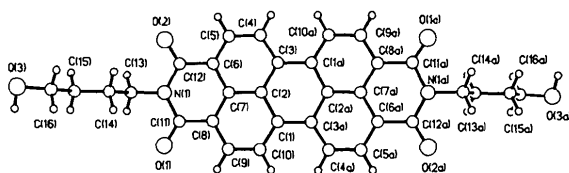


Fig. 1. Molecular structure of (10).

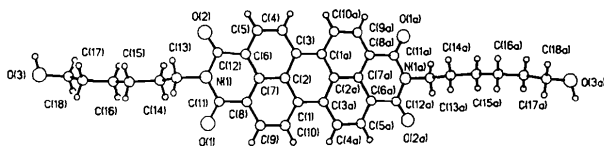


Fig. 2. Molecular structure of (11).

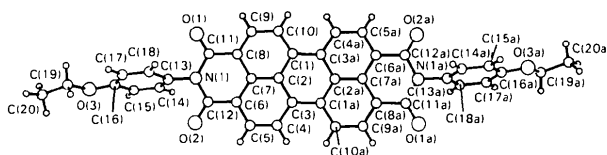


Fig. 3. Molecular structure of (16).

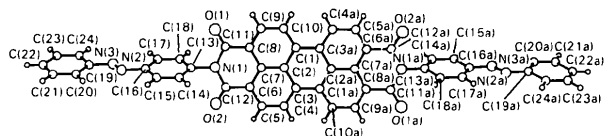


Fig. 4. Molecular structure of (17).

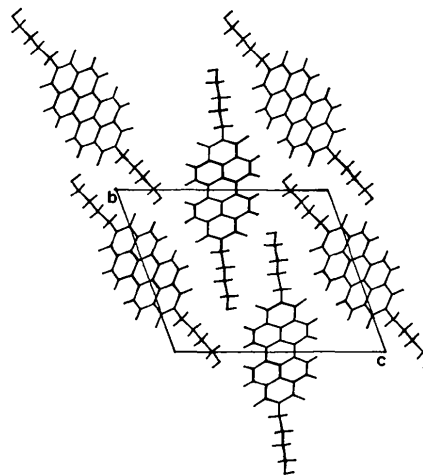


Fig. 5. Crystal packing in (10) projected on the *bc* plane.

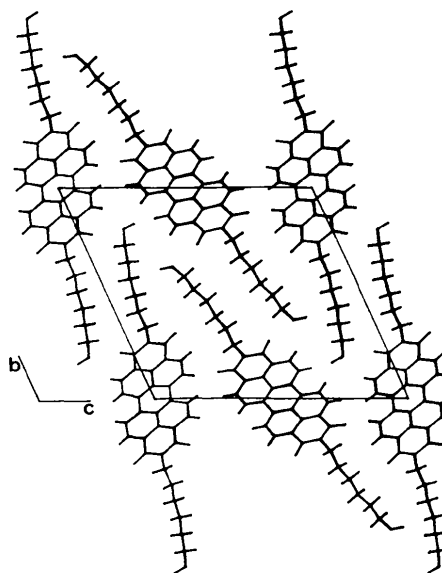
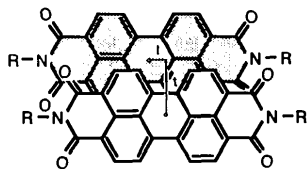


Fig. 6. Crystal packing in (11) projected on the *bc* plane.

In contrast to graphite, the flat perylene skeletons are finite and 'terminated' at each end by a bulky substituent on N. To avoid unfavourable interactions between the stacked molecules in all compounds but (2), a relative longitudinal and transverse shift (see below) is observed. These mutual translations are determined by the steric requirements and the conformation of the bent substituents on N and allow an optimal interlocking of the vicinal side chains. Another



possibility of evading these close intermolecular contacts is realized only in (2) where a relative twisting of the molecules along the stacking direction is found, resulting in a staggered arrangement of the substituents. As a consequence of this translation or rotation respectively, the overlap of the aromatic perylene moieties differs in the various stacks (Fig. 10). This effect gives rise to different electronic interactions and thus to the spread of colours of the perylene pigments in the crystal, whereas the absorption properties of the 'isolated' molecules resemble each other rather closely. Graser & Hädicke (1984) found that the transverse shift of neighbouring molecules in the stack is an essential factor for the differences in colour of the pigments. To derive an empirical correlation between absorption maxima and crystal packing various parameters such as the stacking distance d (Fig. 10), the longitudinal (l) and transverse (t) shifts, and the relative overlap, the squares d^2 , l^2 and t^2 and $(d^2 + l^2 + t^2)^{1/2}$ were submitted, together with λ_{\max} , to a stepwise regression analysis (Draper & Smith, 1981). The

relative overlap of the molecules was determined by projecting them onto each other (along a vector perpendicular to the perylene moiety) and calculating the ratio between the overlapping area of two neighbouring molecules and the size of a single projected molecule. Compound (2) was excluded from the analysis because of its different packing pattern. The multiple regression analysis determines the combination of the above listed variables which gives the best prediction of λ_{\max} . The program starts with a correlation based on one variable. Then a second is included in the analysis and only remains in the regression equation if a significantly better prediction is achieved. In a consecutive process all the various combinations of variables are tested, the following equation giving the best determination of λ_{\max} (confidence intervals in parenthesis):

$$\lambda_{\max} = 9.718(\pm 3.03)l^2 - 82.009(\pm 20.74)t - 21.888(\pm 9.30)d + 735.329$$

($n = 22, r = 0.917, s = 16.242 \text{ nm}, F = 31.83$).

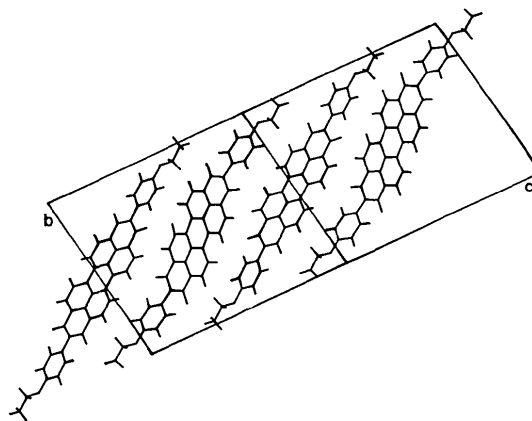


Fig. 8. Crystal packing in (16) projected on the bc plane.

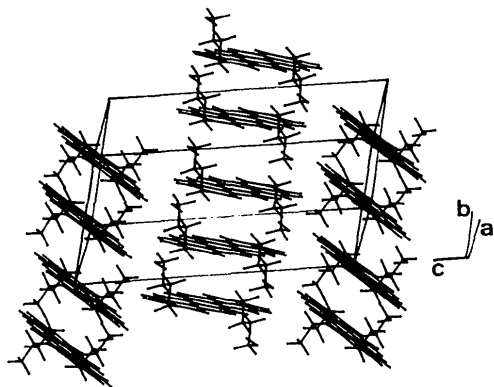


Fig. 7. Crystal packing in (10) viewed nearly parallel to the perylene moiety; best planes through the atoms of the perylene portions in different stacks are inclined at 26° in (10); in (11) this angle is only 6.7° .

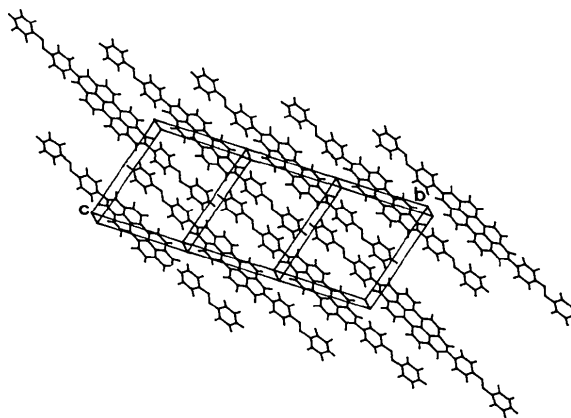


Fig. 9. Crystal packing in (17) viewed nearly parallel to the a axis.

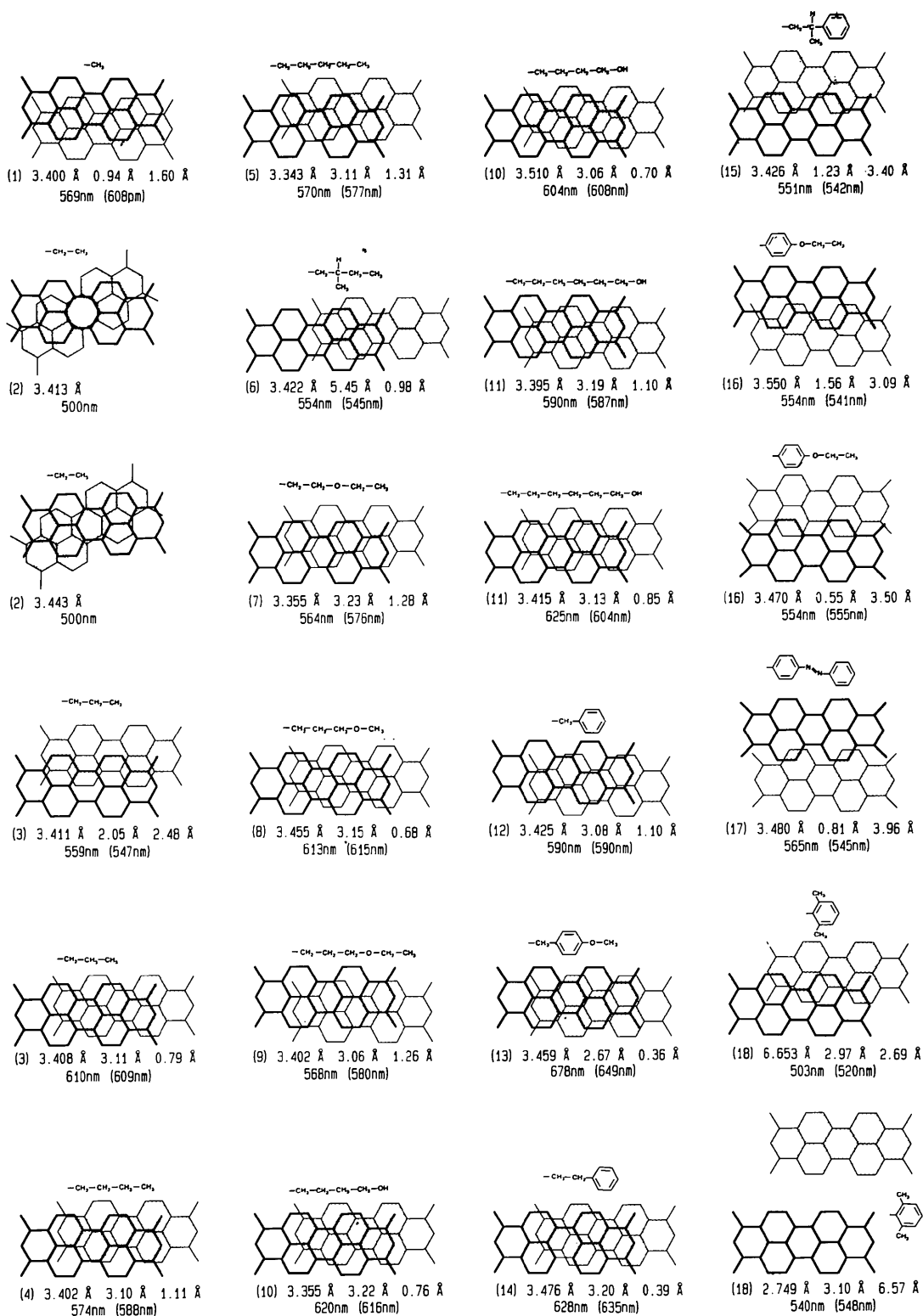


Fig. 10. Stacking pattern of two vicinal perylene moieties in the different pigments projected onto a best plane through the atoms of the fused ring system. For each structure the substituent on N is indicated by its formula; the six numbers below each diagram indicate the compound identification code, the stacking distance (d) between neighbouring molecules, the longitudinal (l) and transverse (t) shifts, the observed solid-state absorption maximum and, in parentheses, λ_{\max} as predicted by the regression analysis. The intermolecular distances are estimated to be correct within ± 0.005 Å for d and ± 0.01 Å for l and t .

A correlation coefficient of $r=0.92$ indicates a reasonably good fit of the assumed model to the experimental data. An s of ± 16.2 nm includes two thirds of the differences between observed and calculated λ values. F is a value used in quantitative structure-activity relationship studies to check the reliability of the model and to discriminate between different parameter equations. The larger its value, the more significant the regression analysis is assumed to be (Fischer test). r , s and F are defined as follows:

$$r = 1 - [\sum(Y_{\text{obs}} - Y_{\text{cal}})^2 / \sum(Y_{\text{obs}} - Y_{\text{mean}})^2]^{1/2}$$

$$s = [\sum(Y_{\text{obs}} - Y_{\text{cal}})^2 / (n - k - 1)]^{1/2}$$

$$F = r^2(n - k - 1) / (1 - r^2)k$$

where Y_{obs} , Y_{cal} , Y_{mean} are the observed, calculated or mean values of λ_{max} , n = the number of data points, and k the number of variables.

The empirical correlation shows that the transverse shift has a more pronounced effect on the variation in colour than the longitudinal shift. The degree of overlap seems to be a minor criterion for the description of the absorption properties since only t , t^2 and l occur in the best-correlation equation.

As a result of the different composition of the asymmetric units and the variety of space groups adopted by compounds (1)–(18), quite different packing arrangements for the global stacks relative to each other are found. However, as the prediction of λ_{max} is achieved reasonably well when only geometrical parameters within a particular stack are considered, it could be concluded that any interactions between different stacks in the crystal are of little or no importance for the absorption properties.

Of greater interest than the empirical correlation of crystal packing with pigment colour is the prediction of crystal packing based on a particular substitution at N. Already a comparison within the homologous series of n -alkyl derivatives (1)–(5) reveals the complexity of this relationship and any prediction appears to be hopeless. No reason seems obvious for the different pattern of (2). Whereas (1), (3), (4), (5) and one of the two symmetry independent molecules of (2) possesses C_i symmetry, the second molecule of (2) resembles C_2 symmetry (Hädicke & Graser, 1986a,b). In (3), two crystallographically independent stacks are formed to which a difference in absorption of 50 nm could be assigned. Accordingly, quite distinct longitudinal and transverse shifts are found. The two independent stacks are due to (3) being in two different conformations. Whereas in one stack the all-*trans* conformation of the n -propyl group is realized, in the second stack the substituent is *gauche*. Compared with the energy difference of 3.3 kJ mol⁻¹ between the *gauche* and *trans* conformation of n -butane, the energy difference between the two different conformations of (3) is assumed to be small. However, the two distinct

arrangements lead to rather different packings. Similar findings hold for the other derivatives (10), (11) and (16) which form symmetry-independent stacks with deviating packing based on slight differences in conformation of the side chain.

Nevertheless, some systematic trends seem apparent from the data (Fig. 11). With regard to the compounds with a linear side chain of more than four members observed in the extended all-*trans* conformation [*i.e.* (5), (7)–(11)], the longitudinal displacement amounts to 3.06–3.23 Å, whereas the transverse translation is found to be appreciably smaller (0.68–1.31 Å). Compounds with a methylene group as a linear spacer between the perylene moiety and a phenyl substituent [(12), (13) and (14)] also reveal a larger longitudinal than transverse shift. In all these compounds the longitudinal shift falls in a small interval, thus for nearly constant l the observed bathochromic shift arises from a decrease in t (see the regression equation).

The phenyl substituent directly bound to the perylene moiety in (16), (17) and (18) is oriented nearly perpendicular to the latter portion. In (16) and (17) the longitudinal translation is appreciably smaller than the transverse shift. With bulky *ortho*-substituents at the

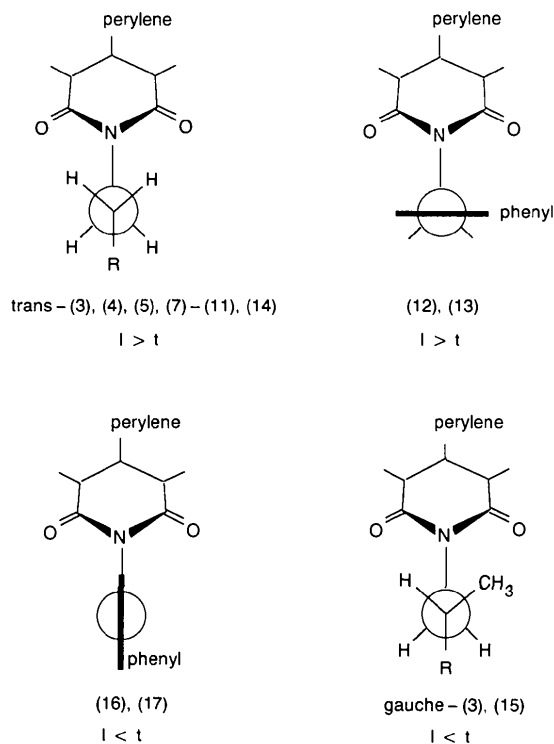


Fig. 11. Correlation between overall shape (steric requirement) of the substituent on N and the ratio between longitudinal (l) and transverse (t) shift. The different compounds belonging to the four groups (expanded aliphatic side chain; benzyl group; directly bound phenyl group; branched side chain) are indicated.

phenyl ring (18) the packing is so strongly perturbed that the stacks are either extremely expanded ($d = 6.65 \text{ \AA}$) or a pronounced transverse shift avoids any overlapping of the molecules (Fig. 11). If branching of the substituent by a methyl group [$\text{CH}_2\text{—CH}(\text{CH}_3)\text{—R}$, (6), (15)] is present, the correlation is less clear cut. In (15) the substituent influences the packing in a similar way as the directly bound phenyl rings in (16) and (17). The observed longitudinal shifts are much smaller than the transverse displacements; accordingly, only a small overlap between neighbouring chromophores is achieved and λ_{max} is found at the lower end.

In (6) the isopentyl group adopts a nonextended conformation, the final methyl group being oriented *gauche* with respect to the rest of the aliphatic C chain. Thus, the overall shape of the substituent is rather bulky. Presumably as a result of these sterical requirements the perylene molecules are strongly shifted (5.45 \AA) in the longitudinal direction against each other, approximately to half of the expansion of the perylene moiety. As a result, the entire substituent is intercalated between two neighbouring perylene portions and any close contacts of the aliphatic substituents on N are avoided. These findings serve to explain why this derivative behaves differently and cannot be classified with the related compounds. Furthermore, there are no apparent reasons why the C_4 chain in the isopentyl substituent does not adopt an energetically favourable *all-trans* conformation. However, the example shows that the molecular conformation of the substituent on N is strongly influenced by molecular packing, or conversely the conformation of the substituent strongly influences molecular packing (what determines what is certainly a question of the mutual energy contributions and the total energy balance).

In the light of these observations the different translations in the two independent stacks of (3) should be reconsidered. Whereas the stack formed by molecules in *all-trans* conformation shows shifts according to the examples with a linear side chain [(5), (7)–(11)], the packing parameters in a stack compiled of *gauche*-(3) are closer to the example with a branched side chain, (15). This fact might be explained by the similar spatial arrangement of the final methyl group in the *gauche*-oriented *n*-propyl substituent (with respect to the perylene moiety) and the orientation of the methyl group in the branched side chain (Fig. 11).

Concluding remarks

The main goal of a systematic investigation is the prediction of properties of new and not yet studied compounds based on the data of known compounds. As this study shows, we are able to describe, to group and

to correlate the packing in various crystal structures with the absorption properties of the solid pigment. Furthermore, we are able to relate the sterical requirements and molecular conformation of a substituent with a particular packing. But rather than the description, a reliable prediction of crystal packing from the structure of an isolated molecule (*e.g.* generated by a force-field calculation) is required. At present our knowledge of the intermolecular interactions and packing energy in crystals is not precise enough. Small differences in energy between conformations of the isolated molecules can add up in the crystal as a result of cooperative effects and give totally different packing [*e.g.* (3)]. For the same reason small incorrect estimations of the different energy contributions to crystal packing could end up in large errors. Accordingly a discussion of packing-energy influences on the present series of compounds was not attempted.

Nevertheless, further systematic studies of closely related compounds and analyses of the data buried in the crystallographic databases provide the challenge of elucidating the mutual energy influences of packing on molecular conformation or *vice-versa* and prediction of crystal packing and thus properties of materials, from the shape and surface (*e.g.* charge distribution) of individual and isolated molecules.

We gratefully acknowledge the help and support of Professor Dr H. Kubinyi (BASF AG) who made his software for the regression analysis available. Furthermore, we are indebted to Mr K. H. Böhn (BASF AG) for his help in collecting and processing the diffractometer data.

References

- BLESSING, R. H., COPPENS, P. & BECKER, P. (1974). *J. Appl. Cryst.* **7**, 488–492.
- DRAPER, N. R. & SMITH, H. (1981). *Applied Regression Analysis*, Wiley Series in Probability and Mathematical Statistics. New York: John Wiley.
- GRASER, F. & HÄDICKE, E. (1980). *Justus Liebigs Ann. Chem.* pp. 1994–2001.
- GRASER, F. & HÄDICKE, E. (1984). *Justus Liebigs Ann. Chem.* pp. 483–494.
- HÄDICKE, E. & GRASER, F. (1986a). *Acta Cryst.* **C42**, 189–195.
- HÄDICKE, E. & GRASER, F. (1986b). *Acta Cryst.* **C42**, 195–198.
- International Tables for X-ray Crystallography* (1974). Vol. IV, pp. 99, 149. Birmingham: Kynoch Press. (Present distributor Kluwer Academic Publishers, Dordrecht.)
- LEHMANN, M. S. & LARSEN, F. K. (1974). *Acta Cryst.* **A30**, 580–584.
- SCHWARZENBACH, D. (1977). *P2 Diffractometer Programs*. Univ. of Lausanne, Switzerland.
- SHELDRIK, G. M. (1978). *SHELXTL. An Integrated System for Solving, Refining and Displaying Crystal Structures from Diffractometer Data* (versions 1979–1983). Univ. of Göttingen, Federal Republic of Germany.
- WILSON, A. J. C. (1949). *Acta Cryst.* **2**, 318–321.